

# Accepted Manuscript

Brain-predicted age in Down Syndrome is associated with  $\beta$ -amyloid deposition and cognitive decline

James H. Cole, Tiina Annus, Liam R. Wilson, Ridhaa Remtulla, Young T. Hong, Tim D. Fryer, Julio Acosta-Cabronero, Arturo Cardenas-Blanco, Robert Smith, David K. Menon, Shahid H. Zaman, Peter J. Nestor, Anthony J. Holland

PII: S0197-4580(17)30124-0

DOI: [10.1016/j.neurobiolaging.2017.04.006](https://doi.org/10.1016/j.neurobiolaging.2017.04.006)

Reference: NBA 9901

To appear in: *Neurobiology of Aging*

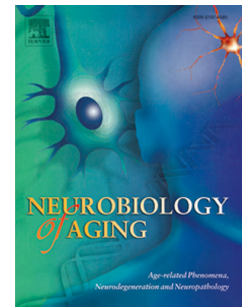
Received Date: 8 December 2016

Revised Date: 9 March 2017

Accepted Date: 9 April 2017

Please cite this article as: Cole, J.H., Annus, T., Wilson, L.R., Remtulla, R., Hong, Y.T., Fryer, T.D., Acosta-Cabronero, J., Cardenas-Blanco, A., Smith, R., Menon, D.K., Zaman, S.H., Nestor, P.J., Holland, A.J., Brain-predicted age in Down Syndrome is associated with  $\beta$ -amyloid deposition and cognitive decline, *Neurobiology of Aging* (2017), doi: 10.1016/j.neurobiolaging.2017.04.006.

This is a PDF file of an unedited manuscript that has been accepted for publication. As a service to our customers we are providing this early version of the manuscript. The manuscript will undergo copyediting, typesetting, and review of the resulting proof before it is published in its final form. Please note that during the production process errors may be discovered which could affect the content, and all legal disclaimers that apply to the journal pertain.



Brain-predicted age in Down Syndrome is associated with  $\beta$ -amyloid deposition and  
cognitive decline

**Authors:**

James H. Cole<sup>a</sup>, Tiina Annus<sup>b</sup>, Liam R. Wilson<sup>b</sup>, Ridhaa Remtulla<sup>c</sup>, Young T. Hong<sup>d</sup>, Tim D. Fryer<sup>d</sup>, Julio Acosta-Cabronero<sup>e</sup>, Arturo Cardenas-Blanco<sup>e</sup>, Robert Smith<sup>d</sup>, David K. Menon<sup>f</sup>, Shahid H. Zaman<sup>b</sup>, Peter J. Nestor<sup>e</sup>, Anthony J. Holland<sup>b</sup>

**Affiliations:**

<sup>a</sup> Computational, Cognitive & Clinical Neuroimaging Laboratory (C3NL), Division of Brain Sciences, Imperial College London, London, UK.

<sup>b</sup> Cambridge Intellectual and Developmental Disabilities Research Group, Department of Psychiatry, University of Cambridge, Cambridge, UK.

<sup>c</sup> University of Birmingham, Birmingham, UK.

<sup>d</sup> Wolfson Brain Imaging Centre, University of Cambridge, UK

<sup>e</sup> German Center for Neurodegenerative Diseases (DZNE), Magdeburg, Germany

<sup>f</sup> Division of Anaesthesia, Department of Medicine, University of Cambridge, UK

**Corresponding Author:**

James H Cole

C3NL, 3<sup>rd</sup> Floor, Burlington Danes Building, Hammersmith Hospital, Du Cane Road,  
London, W12 0NN

[james.cole@imperial.ac.uk](mailto:james.cole@imperial.ac.uk)

## Abstract

(170/170 words)

Individuals with Down Syndrome (DS) are more likely to experience earlier onset of multiple facets of physiological ageing. This includes brain atrophy,  $\beta$ -amyloid deposition, cognitive decline and Alzheimer's Disease; factors indicative of brain ageing. Here we employed a machine learning approach, using structural neuroimaging data to predict age (i.e., *brain-predicted age*) in people with DS (N = 46) and typically developing controls (N = 30). Chronological age was then subtracted from *brain-predicted age* to generate a *brain-predicted age difference* (brain-PAD) score. DS participants also underwent [ $^{11}\text{C}$ ]-PiB positron emission tomography (PET) scans to index levels of cerebral  $\beta$ -amyloid deposition, and cognitive assessment. Mean brain-PAD in DS participants' was +2.49 years, significantly greater than controls ( $p < 0.001$ ). The variability in brain-PAD was associated with the presence and the magnitude of PIB-binding and levels of cognitive performance. Our study indicates that DS is associated with premature structural brain ageing, and that age-related alterations in brain structure are associated with individual differences in the rate of  $\beta$ -amyloid deposition and cognitive impairment.

## Keywords

Down Syndrome; brain ageing; amyloid PET; MRI; machine learning; cognitive decline

## Highlights

- Machine learning of neuroimaging was used to assess brain ageing in Down Syndrome
- Down Syndrome individuals show 'older' brains, based on neuroimaging predictions
- The extent of increased brain 'ageing' related to PET measures of amyloid deposition
- Having an amyloid deposition and an 'older' brain predicted cognitive impairment

## 1. Introduction

Down Syndrome (DS), the result of trisomy 21, results in intellectual disability and a set of characteristic physiological and behavioural traits. In middle adulthood, people with DS also commonly experience clinical symptoms that are normally associated with older age (Covelli, et al., 2016, Devenny, et al., 2005). Whether DS truly results in an acceleration to all aspects of the ageing process is controversial (Zigman, 2013). Nevertheless, skin wrinkles, grey hair and alopecia, visual and auditory decline, hypogonadism, hypothyroidism, osteoporosis and the menopause all occur considerably earlier in people with DS (Covelli, et al., 2016, Zigman, 2013). Beside these physiological manifestations of ageing, evidence also suggests that people with DS experience premature brain ageing. Cognitive decline and subsequent Alzheimer's Disease (AD) occur more frequently and at an earlier age in DS (Devenny, et al., 2000, Holland, et al., 1998, Margallo-Lana, et al., 2007, Wisniewski, et al., 1985). In addition, post-mortem and in-vivo studies show increased cerebral  $\beta$ -amyloid deposition, neurofibrillary tau tangles, brain atrophy and white matter lesions in DS (Annus, et al., 2016, Head, et al., 2016, Lao, et al., 2016, Mann and Esiri, 1989, Nelson, et al., 2011, Roth, et al., 1996, Wisniewski, et al., 1985). All these changes have been associated with the typically ageing brain, albeit at an older age (Braskie, et al., 2010, Fjell, et al., 2009, Jack, et al., 2014, Rodrigue, et al., 2012, Wardlaw, et al., 2013). However, despite this increased prevalence of 'age-like' changes observed in people with DS, the onset of the symptoms of brain ageing and subsequent trajectories of decline show marked variability (Oliver, et al., 1998). While the biological mechanisms underlying these brain changes in DS are likely distinct from normal ageing, their manifestation can still be assessed using the same techniques, such as neuroimaging. Therefore, understanding the relationships between  $\beta$ -amyloid deposition, brain structure and cognitive decline, should help capture these individual differences and allow better prediction of health outcomes.

To measure how brain structure changes with ageing, multivariate machine-learning methods have been developed that allow accurate prediction of chronological age using neuroimaging data (Dosenbach, et al., 2010, Franke, et al., 2010, Mwangi, et al., 2013). This has demonstrated that neuroimaging data can be used to generate an index that quantifies age-related changes to brain volume, which we refer to as 'brain-predicted age'. Accordingly, brain-predicted age, or equivalent, has been used to demonstrate that environmental factors are associated with a person's brain appearing younger or older than

would be expected for their chronological age. Deleterious influences on brain-predicted age include traumatic brain injury (Cole, et al., 2015), obesity (Ronan, et al., 2016), schizophrenia (Koutsouleris, et al., 2013, Schnack, et al., 2016), HIV-infection (Cole, et al., 2017), diabetes (Franke, et al., 2013), mild cognitive impairment and AD (Franke and Gaser, 2012, Gaser, et al., 2013). Conversely, the protective effects of physical exercise, education and meditation (Luders, et al., 2016, Steffener, et al., 2016) have also been reported, indicating that brain-predicted age can deviate outside of the context of atrophy due to brain diseases. The variability in brain-predicted age appears to be a useful way of quantifying individual differences in structural age-related changes to the brain in both disease and the general population.

Here, we sought to establish if people with DS show evidence of premature brain ageing, using neuroimaging to measure brain-predicted age. Furthermore, we considered whether levels of  $\beta$ -amyloid deposition (according to positron emission tomography [PET] imaging), cognitive decline and the manifestation of dementia relate to the levels of 'age-like' changes to brain structure in DS.

## **2. Materials and Methods**

### **2.1. Participants**

The study included  $N = 46$  adults with DS (mean age =  $42.30 \pm 8.73$  years, 25 males/21 females) and  $N = 30$  typically developing adults as a control group (mean age =  $46.23 \pm 9.75$ , 16 males/14 females). All 76 individuals underwent MRI scans, while the DS group also underwent PET scans. Data on these individuals have been previously reported (Annus, et al., 2016). All DS participants had previously received a clinical diagnosis of DS based on having the characteristic phenotype, while a proportion ( $N = 33$ ) were karyotyped to confirm the presence of trisomy 21. Participants were screened to ensure that they had no contraindications to MRI and PET scanning. Ethical approval for the study was granted by the National Research Ethics Committee of East of England and the Administration of Radioactive Substances Advisory Committee (ARSAC). Written consent was obtained from all adults with DS with the capacity to consent. For participants lacking the capacity to consent the procedures set out in the England and Wales Mental Capacity Act (2005) were followed. These 76 individuals comprised the brain-predicted age test set.

To define a multivariate model of healthy brain structure across the lifespan, data were collated from publicly-available sources. This included  $N = 2001$  typically developing,

healthy individuals (mean age =  $36.95 \pm 18.12$ , age range 18-90 years, 1016 males/985 females), who comprised the brain-predicted age training set (see Supplementary Table 1). All training set participants were screened locally to exclude individuals with major neurological or psychiatric diagnoses, a history of head trauma or major physical health problems, as per local study protocols. Each contributing study was granted ethical approval for data collection and subsequent data-sharing. Informed consent was obtained at each local study site in accordance with local guidelines.

## **2.2. Clinical and neuropsychological assessment**

All DS participants were assessed for dementia using an informant interview; the Cambridge Examination for Mental Disorders of the Elderly-Down Syndrome version (CAMDEX-DS), adapted from the original CAMDEX for diagnosing dementia specifically in DS (Ball, et al., 2004). These informant interviews were conducted by trained researchers at the University of Cambridge. Subsequently, an experienced clinician (SHZ), who was blinded to participant identity, used interview transcripts to assign DS participants to one of three discrete categories: cognitively stable, cognitive decline or dementia. Classification of dementia was in line with established criteria (International Classification of Disease 10). Cognitive decline was defined as evidence of cognitive impairment in one or more cognitive domains without fulfilling the full criteria for dementia. As part of the CAMDEX, all participants in the DS group underwent the Cambridge Cognitive Examination (CAMCOG - Holland, et al., 1998). The CAMCOG collates functioning across a range of cognitive domains and generates a continuous measure of cognitive function, where higher scores indicate higher levels of cognitive performance. Three DS participants were unable to complete the CAMCOG assessment, due to having advanced symptoms of dementia.

## **2.3. Apolipoprotein E genotyping**

DS participants supplied blood samples that were processed to determine genotypes for apolipoprotein E (APOE). Peripheral blood samples were stored in EDTA tubes and the DNA extracted using standard methods. The DNA was genotyped for ApoE, using primers pairs to amplify by PCR the region containing the Arg/Cys polymorphism at codons 112 and 158 of the APOE gene. Standard polymerase chain reaction (PCR) was performed using PCR mix (Bioline) using Taq polymerase to unambiguous typing of all homozygotic and heterozygotic isoform combinations. For analysis purposes, APOE genotype was used to define a binary categorisation of each participant as either an e4 carrier or not an e4 carrier.

APOE data were missing for N = 6 DS participants, from whom blood samples could not be collected.

## 2.4. Neuroimaging data acquisition

Full details of the PET acquisition protocol have been previously reported (Annus, et al., 2016). In brief, PET data were acquired using a GE Advance scanner (General Electric Medical Systems, Milwaukee, USA) to measure levels of [ $^{11}\text{C}$ ]-Pittsburgh compound B (PiB) uptake across the brain. [ $^{11}\text{C}$ ]-PiB was injected as a bolus via a catheter and data were acquired for 90 minutes post-injection. Fifty-eight frames were acquired as follows: 18 x 5 seconds, 6 x 15 seconds, 10 x 30 seconds, 7 x 60 seconds, 4 x 150 seconds, 13 x 300 seconds. Sinogram data were then reconstructed, resulting in a voxel size of 2.34 x 2.34 x 4.25 mm. Visual inspection of the PET data was conducted to ensure that there were no major head movements or other artefacts present.

Structural images were T1-weighted MRI scans, acquired for the DS and control groups using the same Siemens Verio 3T scanner (Siemens AG, Erlangen, Germany). A magnetisation-prepared rapid gradient echo (MPRAGE) sequence was used, with the following parameters: TR = 2300 ms, TE = 2.98 ms, TI = 900 ms, flip angle = 9°, matrix dimension = 256 x 240. The protocol acquired 176 axial slices of 1mm thickness, resulting in voxels of 1mm<sup>3</sup>. Parallel acceleration was not enabled.

High-resolution T1-weighted data were also used from the training dataset, collated from previous studies. All training data were acquired at either 1.5T or 3T using standard T1-weighted sequences (e.g., MPRAGE, SPGR, T1-FFE).

## 2.5. PiB binding analysis

To measure [ $^{11}\text{C}$ ]-PiB uptake levels across the brain, non-displaceable binding potential ( $\text{BP}_{\text{ND}}$ ) was calculated for different cerebral regions of interest (ROIs). This process involved two stages; the delineation of ROIs using T1-MRI and then the extraction of mean PiB  $\text{BP}_{\text{ND}}$  levels for each ROI from the PET data (as per Annus, et al., 2016). To delineate cortical ROIs, a customised Brodmann atlas, registered to the Colin27 T1 template, was warped to a study-specific T1 template. This process was achieved using the Advanced Normalisation Tools (ANTS - Avants, et al., 2011) and involved skull-stripping, affine global registration and an iterative non-linear local registration procedure to generate the study specific template and register the atlas to the template. The Colin27-Brodmann atlas was then resampled to the study template space using nearest neighbour interpolation. Sub-

cortical ROIs were also included, derived using FSL FIRST (Patenaude, et al., 2011), resulting in a total of 30 ROIs. FIRST analysis was conducted in participant native space, before being resampled into study template space, again using nearest neighbour interpolation for discrete ROI images. To reduce the influence of partial volume effects (PVE), T1 images were segmented (i.e., tissue classified) using SPM12 (University College London, London, UK) to generate grey matter (GM), white matter (WM) and cerebrospinal fluid (CSF) probability images. These images were also warped to the study-specific templates using the ANTS transformations calculated as above.

PET data were also normalised to the study-specific template. This involved initially realigning the dynamic PET time-series and then averaging them across time using SPM12. These mean images were then rigidly registered to their corresponding native T1 images (which had been bias-field corrected), using ANTS. Then, by combining together the PET-T1 native and T1-study template transformations, PET images were normalised to the study template using a single resampling step, via trilinear interpolation.

Next, regional PiB BP<sub>ND</sub> values were calculated, using PET data, cortical and sub-cortical ROIs and tissue probability masks, all in study template space. For each ROI, thresholded at ≥65% GM probability, time-activity-curves (TACs) were extracted from the normalised PET data. Tissue-input kinetic modelling was then carried out, using the superior cerebellum as a reference region (thresholded to ≥90% GM probability). As a further step to reduce PVEs, each TAC was divided by 1-CSF probability value in each voxel. The final BP<sub>ND</sub> per ROI was then calculated using a basis function version of the simplified reference tissue model (Gunn, et al., 1997).

To ascertain whether an individual's PET data indicated that they had abnormal levels of PiB binding (i.e., PiB-status), indicative of fibrillary  $\beta$ -amyloid deposition, our previously outlined procedure was used (Annus, et al., 2016). This entailed defining a bimodal distribution of striatal (i.e., caudate and putamen) PiB BP<sub>ND</sub> levels. Individuals with striatal PiB BP<sub>ND</sub> <1 standard deviation (SD) from 0 were defined as PiB-negative, while individuals with striatal PiB BP<sub>ND</sub> ≥1 SD from 0 were defined as PiB-positive. Subsequently, regional PiB BP<sub>ND</sub> was defined as normal or abnormal per participant, based on the distribution of PiB BP<sub>ND</sub> for a given region in the PiB-negative group. Abnormal PiB BP<sub>ND</sub> was defined as ≥2 SDs from the PiB-negative group mean. Finally, the total number of ROIs defined as

abnormal was summed per participant. Notably, individuals in the PiB-negative group did not show any evidence of abnormal PiB BP<sub>ND</sub> in non-striatal ROIs. In addition to classifying ROIs based on PiB BP<sub>ND</sub>, the mean PiB BP<sub>ND</sub> across all cortical ROIs was calculated.

## 2.6. Brain-predicted age calculation

An overview of the brain-predicted age calculation procedure is presented in Figure 1. All structural images were pre-processed using SPM12. Images were bias corrected and segmented into GM, WM and cerebrospinal fluid (CSF) using SPM *Segment*. Visual quality control was carried out at this stage to ensure the accuracy of image segmentation; all images were included for both groups. Segmented images for GM and WM were then non-linearly registered to a custom template, based on the training dataset, using SPM *DARTEL* (Ashburner, 2007). Finally, images were affine registered to MNI152 space (voxel size = 1.5mm<sup>3</sup>) and resampled using modulation to retain volumetric information and smoothed with a 4mm full-width half-maximum Gaussian kernel. Summary measures of brain volumes were also generated for GM, WM, CSF and intracranial volume (ICV).

Brain-predicted ages were generated as previously outlined (Cole, et al., 2015), using the Pattern Recognition for Neuroimaging Toolbox (PRoNTo v2.0, [www.mnl.cs.ucl.ac.uk/pronto](http://www.mnl.cs.ucl.ac.uk/pronto)) software package. First, a model of healthy brain ageing was defined using brain volumetric maps from the training dataset (N = 2001) as follows: Spatially normalized images were converted to vectors and the resulting GM and WM vectors were concatenated for each individual. A linear kernel representation of these data was derived by calculating an  $N \times N$  similarity matrix, where each point in the matrix was the dot product of two participants' image vectors. A Gaussian Processes regression model was then defined, with chronological age as the dependent variable and three-dimensional brain volumetric image data (in similarity matrix form) as the independent variables.

Predictions for all training participants were generated using ten-fold cross-validation, whereby the data were randomly divided into 10 folds, each comprising 10% of the participants. The model was then re-trained using 9 folds of the data and age predictions were made for data in the 'left-out' fold. This procedure was iterated so that all folds were left-out in turn, resulting in unbiased (i.e. independent) age predictions for each participant. Model accuracy was expressed as the correlation between age and brain-predicted age (Pearson's  $r$ ), total variance explained ( $R^2$ ), mean absolute error (MAE) and root mean

squared error (RMSE). Statistical significance of this model was assessed using permutation testing ( $n = 1,000$ ).

Next, the coefficients from the full training model ( $N = 2001$ ) were applied to the test data (i.e., DS participants and controls), to generate unbiased brain-predicted ages. Finally, brain-predicted age difference (brain-PAD) scores were calculated for each individual in the DS and control groups by subtracting chronological age from brain-predicted age. Hence, a positive brain-PAD score indicates that the individual's brain is predicted to be 'older' than their chronological age. Brain-PAD scores were subsequently used for further analysis to index relative structural brain ageing.

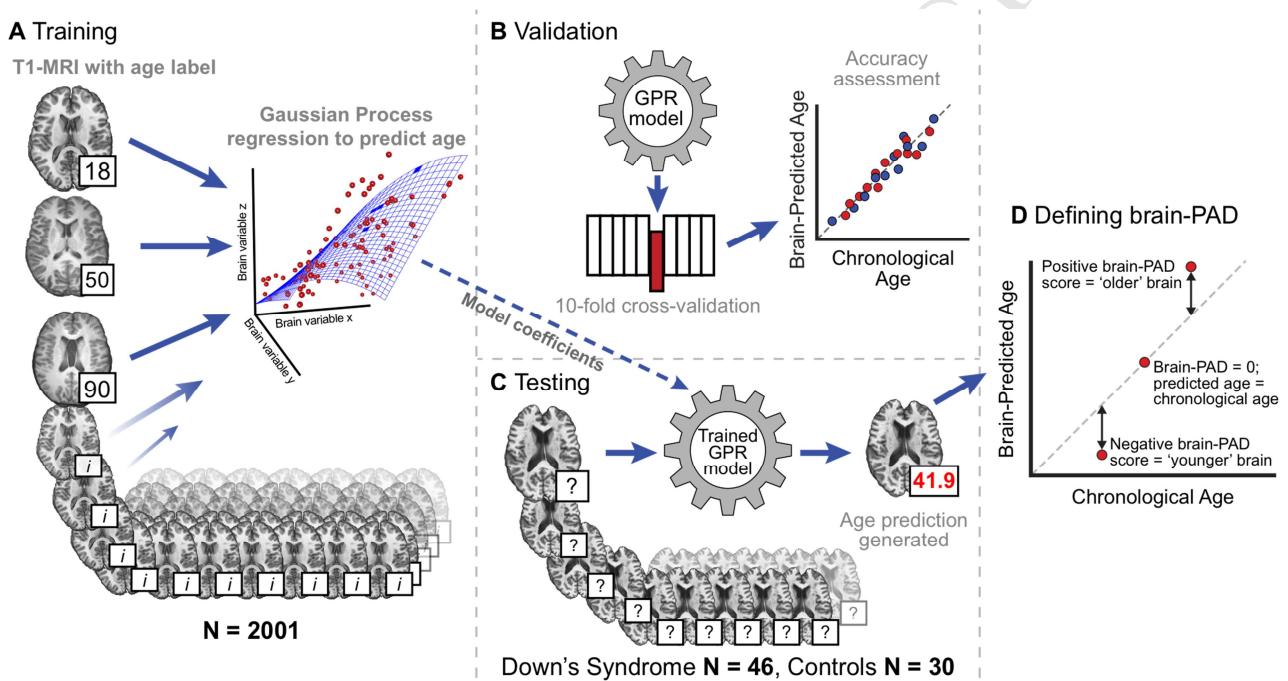


**Figure 1. Overview of the brain-predicted age analysis pipeline**

Illustration of the methods used to generate brain-predicted ages. 3D T1-weighted MRI scans were segmented into grey matter (GM) and white matter (WM) before being normalized to common space using non-linear image registration. Normalized GM and WM images were concatenated and converted into vectors for each participant. These vectors were then projected into an  $N \times N$  similarity matrix based on vector dot-products. A) Once in similarity matrix form the training participants' data were used as predictors in a Gaussian Processes regression (GPR) model with age as the outcome variable. B) Model accuracy was assessed in a 10-fold cross-validation procedure, comparing brain-predicted age with original chronological age labels. C) Model coefficients learned during training were then applied to the data from DS participants and controls to generate brain-predicted ages. D) A metric to summarize the variation in brain-predicted age was defined; the brain-predicted age difference (brain-PAD; brain-predicted age - chronological age).

## 2.7. Statistical analysis

Using brain-PAD values, further statistical analysis was conducted to compare experimental groups and assess relationships between variables. Data were assessed for normality and

parametric tests deemed appropriate for use. Fisher's exact tests were used to compare the frequencies of categorical variables, Pearson's correlations were used to relate continuous variables and t-tests were used to compare means between groups. A linear regression model was run with brain-PAD as the outcome variable and group as the predictor, to compare brain-PAD between DS participants and controls. Linear regression was also used to compare ICV between groups. To establish whether brain-PAD predicted characteristics of the DS participants, logistic regressions for categorical outcomes variables (PiB-status, CAMDEX classification) and linear regressions for continuous outcomes variables (mean BPND, number of PiB-abnormal ROIs, CAMCOG score) models were run, with age as a covariate. All statistical analysis of brain-PAD was conducted using R v3.3 (R Core Team, 2015).

### 3. Results

#### 3.1. Cohort description

Compared to controls, DS participants were trending towards being younger (Table 1,  $p = 0.08$ ), while the ratio of males to females was similar between groups ( $p = 0.96$ ). DS participants who were positive for PiB-binding were older than PiB-negative counterparts ( $p < 0.001$ ), had higher rates of cognitive decline and dementia according to CAMDEX classification ( $p < 0.001$ ), though similar levels of cognitive performance, according to the CAMCOG assessment ( $p = 0.33$ ). There was no relationship between PiB-status and sex ( $p = 0.78$ ).

**Table 1. Characteristics of Down Syndrome participants and controls**

	DS (all)	DS PiB-positive	DS PiB-negative	Controls
<b>N</b>	46	19	27	30
<b>Mean age (years)</b>	42.3 (8.73)	49.68 (6.45)	37.11 (5.95)	46.23 (9.75)
<b>Age range (years)</b>	28-65	39-65	28-48	30-64
<b>Sex (male/female)</b>	25/21	11/8	14/13	16/14
<b>CAMDEX classification (stable, declining, dementia)</b>	31/6/9	7/5/7	24/1/2	-
<b>CAMCOG score</b>	74.37 (20.01)	70.19 (22.98)	76.85 (18.03)	-
<b>APOE genotype (e2/e3, e2/e4, e3/e3, e3/e4/missing)</b>	8/2/20/10/6	4/1/6/5/3	4/1/14/5/3	-

Values presented in the table are either N, or in mean (standard deviation) form.

### 3.2. Age can be accurately predicted using neuroimaging

The machine-learning model accurately predicted chronological age in the training dataset, based on T1-weighted MRI. Ten-fold cross validation resulted in a correlation between brain-predicted age and chronological age of  $r = 0.94$ , ( $p = 0.001$ , corrected after 1,000 permutations) and explained 88% of the variance ( $R^2$ ). The MAE of prediction = 5.02 years and the RMSE = 6.31 years. This training stage validated our model of brain-predicted age for use in predicting age with neuroimaging data in the test set, comprising DS participants and controls.

### 3.3. Down Syndrome is associated with increased brain-predicted age difference

Brain-PAD in DS participants was significantly greater than controls ( $b = 7.69$  [95% confidence intervals = 4.3, 11.1],  $SE = 1.72$ ,  $t = 4.46$ ,  $p < 0.001$ , Figure 2A). Mean brain-PAD in the DS group was 2.49 years ( $SD = 8.25$ ), while in the control group mean brain-PAD was -5.20 years ( $SD = 5.67$ ). Brain-PAD in the DS group was significantly greater than the training set mean ( $t = 2.04$ ,  $p = 0.04$ ). Brain-predicted age was significantly correlated with chronological age in both DS participants ( $r = 0.72$ ,  $p < 0.001$ ) and in controls ( $r = 0.91$ ,  $p < 0.001$ , Figure 2B). There were no differences in prediction accuracy between groups ( $p = 0.91$ ), with the MAE in DS = 6.65 ( $SD = 8.20$ ) years and in controls MAE = 6.46 ( $SD = 5.67$ ) years. The RMSE = 8.53 in DS and 7.62 in controls.

As head size has been shown to differ between individuals with DS and typically developing individuals, we also investigated the influence of ICV on brain-PAD. Indeed, DS participants did have reduced ICV relative to controls (DS mean = 1.19L ( $SD = 0.11$ ), control mean = 1.42L ( $SD = 0.14$ ),  $b = -0.02$ ,  $SE = 0.03$ ,  $t = -7.89$ ,  $p < 0.001$ ). However, ICV was not significantly correlated with brain-PAD in the DS group ( $r = -0.04$ ,  $p = 0.77$ ) or the control group ( $r = 0.09$ ,  $p = 0.62$ ). There were no sex differences in brain-PAD in either the DS group ( $t = 0.66$ ,  $p = 0.51$ ) or the control group ( $t = 1.00$ ,  $p = 0.32$ ). APOE genotype did not significantly influence brain-PAD ( $t = -1.63$ ,  $p = 0.11$ ).

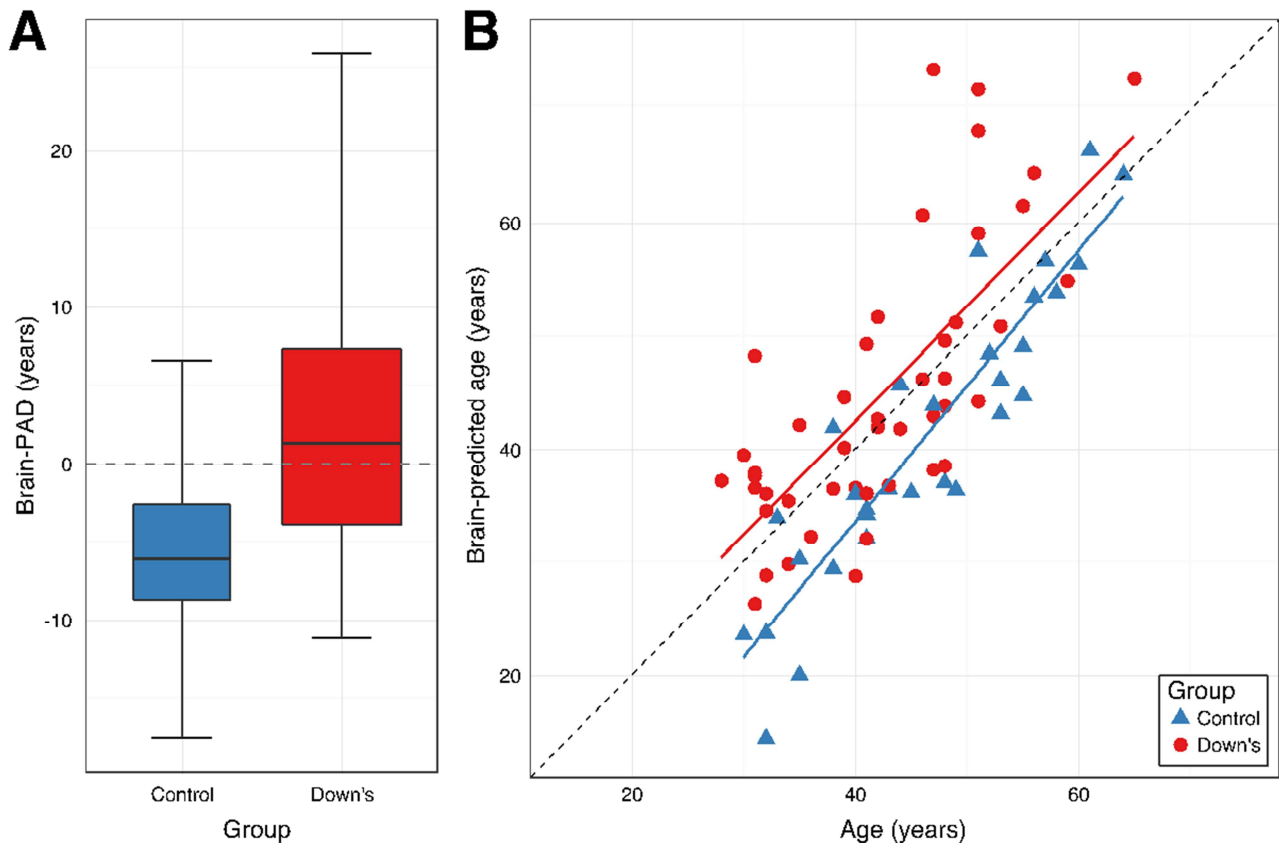


**Figure 2. Brain-predicted age in individuals with Down Syndrome and controls**

A) Box plot of brain-PAD (years) according to group, showing DS participants (red box) and controls (blue box). Whiskers (i.e., bars) on the boxplots represent the absolute range of data points for each group. B) Scatterplot of age (x-axis) and brain-predicted age (y-axis). Red circles indicate DS participants and blue triangles controls. Plotted are linear regression lines representing a linear fit of age regressed onto brain-predicted each, coloured according to group (DS = red line, control = blue line).

### 3.4. Brain-predicted age increases are associated with increased PiB binding potential

Within the DS group, 19 individuals were classified as PiB-positive based on PET data, while 27 individuals showed no evidence of abnormal PiB binding (PiB-negative). The mean cortical PiB BP<sub>ND</sub> across PiB-positive individuals =  $0.36 \pm 0.22$ , while the median number of ROIs showing abnormal PiB levels in these individuals was 28 (range 1-30). Brain-PAD significantly predicted PiB-status in DS participants ( $b = 0.20$  [95% confidence intervals = 0.03, 0.44],  $SE = 0.10$ ,  $z = 1.98$ ,  $p = 0.048$ ), as did chronological age ( $b = 0.42$ ,  $SE = 0.14$ ,  $z = 3.11$ ,  $p = 0.002$ ), in a logistic regression model. The group mean brain-PAD scores were  $5.29 \pm 9.41$  years in PiB-positive DS participants and  $0.52 \pm 6.84$  years in PiB-negative DS participants (Figure 3A). Brain-predicted age was significantly correlated with chronological age in PiB-positive individuals ( $r = 0.54$ ,  $p = 0.02$ ), though this relationship was only

borderline in PiB-negative DS participants ( $r = 0.32$ ,  $p = 0.08$ , Figure 3B). Brain-PAD significantly predicted both mean cortical PiB  $BP_{ND}$  ( $b = 0.008$ ,  $SE = 0.003$ ,  $t = 2.78$ ,  $p = 0.001$ ) and the number of ROIs showing abnormal PiB levels ( $b = 0.46$ ,  $SE = 0.14$ ,  $t = 3.40$ ,  $p = 0.001$ ), when covarying for chronological age (which was also significantly related to both quantitative PiB measures,  $p < 0.05$ ) in DS participants.

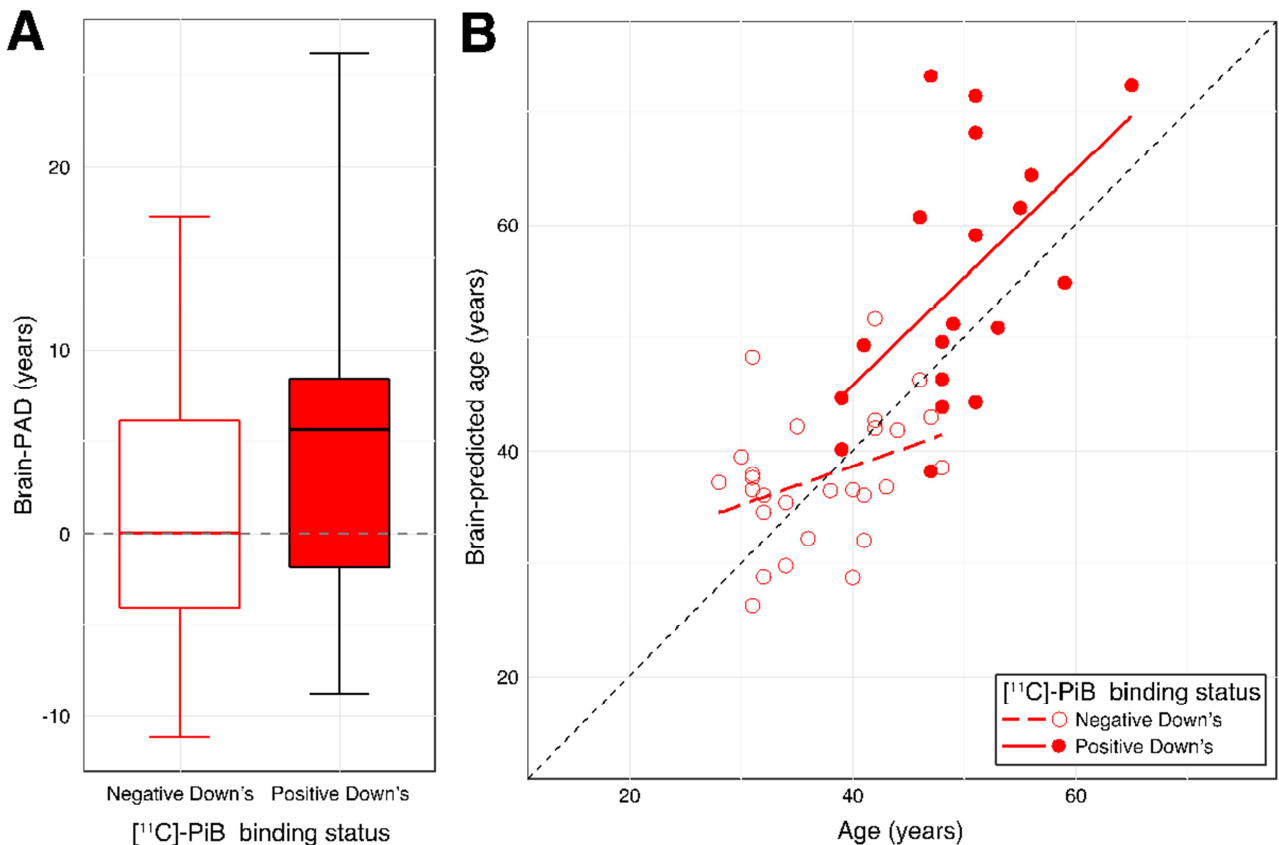


**Figure 3. Brain-predicted age in individuals with Down Syndrome, according to [ $^{11}\text{C}$ ]-PiB status**

A) Box plot of brain-PAD (years) according to [ $^{11}\text{C}$ ]-PiB status in DS participants. PiB-positive (red box) and PiB-negative (white box). Whiskers (i.e., bars) on the boxplots represent the absolute range of data points for each group. B) Scatterplot of age (x-axis) and brain-predicted age (y-axis). Filled red circles indicate PiB-positive DS participants and open red circles PiB-negative DS participants. Plotted are linear regression lines representing a linear fit of age regressed onto brain-predicted each, coloured according to group (PiB-positive = solid red line, PiB-negative = dashed red line).

### 3.5. Brain-predicted age increases are related to poorer cognitive performance in PiB-positive individuals

When considering all DS participants together, there was a significant effect of brain-PAD on CAMCOG score ( $b = -0.80$ ,  $SE = 0.35$ ,  $t = -2.24$ ,  $p = 0.03$ ), whereby higher brain-PAD was associated with worse performance on the CAMCOG assessment. However, when considering PiB-status in the model, there was a significant interaction between brain-PAD and PiB-status ( $b = -1.75$ ,  $SE = 0.72$ ,  $t = -2.42$ ,  $p = 0.02$ ), when predicting CAMCOG score

(Figure 4). This indicates that in PiB-positive DS participants there is a strong negative relationship between brain-PAD and CAMCOG score, while in PiB-negative DS participants, there is no such relationship. This was despite there being no significant difference in CAMCOG score based on PiB-status, as noted above. Age was not included as a covariate in these analyses as age was not related to CAMCOG score ( $p = 0.33$ ). Ordinal logistic regression analysis indicated that brain-PAD score did not significantly predict CAMDEX classification, either with or without PIB-status as an additional covariate ( $p = 0.73$ ;  $p = 0.72$ ). Interestingly, when excluding DS individuals with declining or dementia ratings from the CAMDEX (i.e., limiting the analysis to cognitively stable individuals,  $N = 31$ ), there was still a significant effect of group on brain-PAD ( $b = 7.34$ ,  $SE = 1.75$ ,  $t = 4.19$ ,  $p < 0.001$ ). We then further investigated the relationship between PIB-status and CAMDEX classification, though we collapsed the CAMDEX into a binary classification of stable vs. not stable (i.e., declining or dementia). There was a significant relationship between PIB-status and CAMDEX ( $p < 0.001$ ), as DS individuals were more likely to be stable if there were PIB-negative, and more likely to be declining if they were PIB-positive (see Supplementary Table 2). However, there was no main effect of these sub-groups on brain-PAD ( $p = 0.23$ ).

Finally, we considered how the magnitude of PIB-binding (measured by mean  $BP_{ND}$ ) and brain-PAD related to cognitive impairment (i.e., CAMCOG score). A linear regression model including mean  $BP_{ND}$  and brain-PAD as predictor variables and CAMCOG score as the outcome was significant ( $p = 0.025$ ) and explained ( $R^2 =$ ) 12.6% of the variance in CAMCOG.

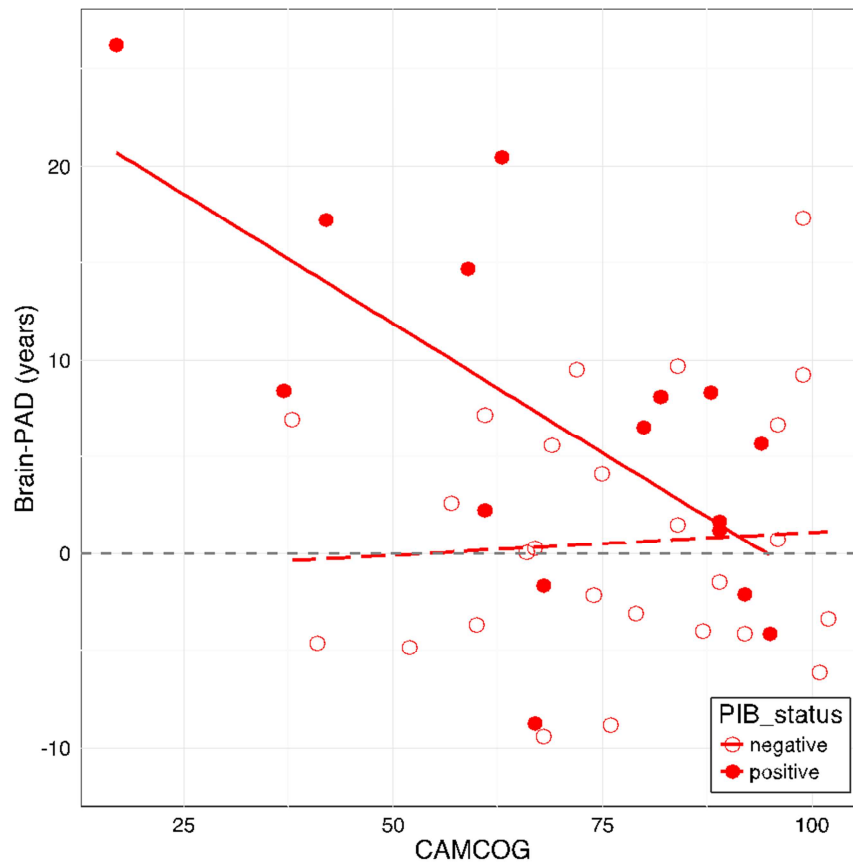


**Figure 4. Cambridge Cognitive Battery performance relates to Brain-PAD, according to [11C]-PiB status**

Scatterplot of CAMCOG score (x-axis) against brain-PAD (y-axis) in DS participants. Filled red circles indicated PiB-positive individuals, while open red circles indicate PiB-negative individuals. Plotted are linear fit lines of CAMCOG score regressed onto brain-PAD for each group (PiB-positive: solid line; PiB-negative: dashed line), to illustrate the interaction between brain-PAD and PiB-status in predicting CAMCOG score.

#### 4. Discussion

Individuals with DS showed increased brain-PAD scores, indicating that the three-dimensional patterns of brain volume associated with DS resembled that of healthy individuals on average 2.49 years older. Moreover, the effect of DS on brain-PAD was an adjusted increase of 7.69 years, compared to scanner-matched, typically developing controls. There was considerable variability observed in brain-PAD in DS participants. Notably, this variability related to measures of amyloid deposition, indexed by [ $^{11}\text{C}$ ]-PiB PET imaging and to cognitive decline, according to CAMCOG assessment. The relationship between brain-PAD and CAMCOG score was observed only in individuals with evidence of amyloid deposition, indicating that changes in brain structure and cognitive performance may be linked to the deleterious build-up of amyloid in DS.

This is the first application of a neuroimaging-based ‘brain-predicted age’ index in people with DS. The observed increased brain-PAD supports the idea that the long-term consequences of DS include premature ‘age-like’ changes to the structure of the brain. Previously, studies have shown lower brain volumes or abnormal cortical thickness in DS (Koran, et al., 2014, Mullins, et al., 2013, Pinter, et al., 2001, Romano, et al., 2016, Teipel, et al., 2004) as well as a correlation between age and brain volume in individuals with DS, not seen in controls (Beacher, et al., 2010, Krasuski, et al., 2002). While these results have been used to indirectly infer the presence of ‘accelerated’ brain ageing in DS, our machine-learning method provides a more direct approach of quantifying age-related changes to brain structure, by way of reference to a large lifespan training sample. Moreover, this technique captures voxelwise variation in brain volumes, incorporating higher-resolution data into the prediction, and is more appropriate for making individualised predictions, rather than relying on group-average trends. Crucially, however, cross-sectional analysis can only suggest ‘premature’ or ‘accentuated’ brain ageing, which is a limitation of the current analysis. Longitudinal studies are necessary to determine whether these age-like changes to brain structure are static or are accelerating over time.

Various mechanisms could underlie the increase in brain-PAD observed in DS. One candidate is the triplication of the amyloid precursor protein (APP) gene, found on chromosome 21, which results in increased levels of APP (Rumble, et al., 1989). As APP is necessary for amyloid protein production, its overexpression may result in increased amyloid levels and subsequent development of neuritic plaques, a key risk factor for AD. Hence, APP triplication may explain the earlier onset and higher prevalence of AD in DS. In our study, PET-derived measures of the magnitude of fibrillary  $\beta$ -amyloid deposition were related to brain-PAD in DS participants, when accounting for the age-dependence of PiB levels (Hartley, et al., 2014). Conversely, brain-PAD did not relate to CAMDEX classification, though interestingly, a model containing brain-PAD and mean PIB-binding significantly predicted CAMCOG scores. This highlights the convergence of amyloid-deposition, structural brain changes and cognitive impairment in DS. While determining causality from these cross-sectional is not possible, our findings suggests that the accumulation of fibrillary  $\beta$ -amyloid may be a precursor to the loss of brain tissue volume and cognitive changes, with dementia symptoms manifesting later in the timeline of neurodegenerative processes.

Other factors that potentially explain premature brain ageing in DS include the triplication of other genes on chromosome 21, such as SOD-1 and SLC5A3, involved in response to oxidative stress and in moderating cerebral myo-inositol levels, respectively (Beacher, et al., 2010). Evidence also suggests that mitochondrial dysfunction occurs in DS in both peripheral and central cells (Phillips, et al., 2013, Tiano and Busciglio, 2011). Maintenance of mitochondrial functions, particularly the production of ATP, is crucial to many aspects of cellular function, and mitochondrial changes have been implicated in aspects of ageing (reviewed by Lopez-Otin, et al., 2013). Plausibly, mitochondrial dysfunction in neurons and astrocytes caused by trisomy 21 could impact on the metabolism of APP (Busciglio, et al., 2002) and result in a cascade of downstream affects that prematurely age brain structure in DS.

From an environmental perspective, physical health and dietary factors, as evidenced by the increased rates of obesity (Melville, et al., 2005), may have indirect effects on physiological 'wear-and-tear'. This could contribute to multiple aspects of ageing in DS, including the brain. Cerebrovascular factors, such as cerebral amyloid angiopathy and micro-haemorrhages, perhaps as a result of persistent neuroinflammation (Wilcock, et al., 2016), may also be involved. Such factors are thought to contribute to brain atrophy outside of the context of DS (Chowdhury, et al., 2011, Muller, et al., 2011), however are unlikely to be entirely independent of the genetic and environmental issues discussed above. A cluster of inter-related risk factors appears to be present in DS, negatively impacting the neural milieu and hence increasing the rate of tissue volume loss normally associated with ageing.

Ours is not the first study to assess tissue-specific measure of ageing in DS. Previously, shortened lymphocyte telomere length has been reported in people with DS (Jenkins, et al., 2006, Vaziri, et al., 1993) and shorter telomeres have been associated with cognitive decline and dementia status in DS (Jenkins, et al., 2010, Jenkins, et al., 2016). Indices of age-associated oxidative stress have also been reported as elevated in DS (Jovanovic, et al., 1998). Recently, Horvath and colleagues (2015) reported 'accelerated' epigenetic ageing in people with DS, using a multivariate method to predict age based on DNA methylation status in blood, buccal cells and brain tissue. This indicates that premature age-like changes are occurring at a molecular level in individuals with DS, of which the reduced brain volume detected by brain-predicted age, may be a macroscopic manifestation. Interestingly, the 'residual' approach adopted by Horvath and colleagues, which essentially sets the control group mean to zero, resulted in an average effect of DS

equivalent to 6.6 years accelerated ageing. Taking the same approach here, we see an effect of a similar magnitude, 7.4 years of added ageing. In future studies, it could prove informative to combined multiple ageing biomarkers (e.g. telomere length, epigenetic clock and brain-predicted age) to assess whether predictions of cognitive decline and dementia risk can be improved.

A potential criticism of neuroimaging models of brain-predicted age is that results could be driven by deviation from normality, as opposed to divergence along a specifically age-related trajectory. While such deviations may occur in neurological conditions, such as stroke or encephalopathy, this is not the case in DS. Brain atrophy in DS is likely to be gradual and cumulative, caused by factors such as increased amyloid deposition or secondary effects of exposure to abnormal neurodevelopment, rather than resulting from a one-off insult. While DS brains have been shown to be abnormal in size and morphology (Annus, et al., 2017, Wang, 1996), brain-PAD scores did not correlate with ICV, nor does ICV correlate with brain-PAD in healthy individuals, so global size differences do not appear to be driving the results. Distinctive brain morphology in DS also did not seem to influence our findings as we observed no differences in the MAE of age-prediction in the DS and control groups; age prediction accuracy was not hindered by any morphological features of DS. While in general it can be difficult to distinguish between ageing effects and disease effects in conditions such as DS, the fact that increased brain-PAD was seen when limiting the analysis to cognitively stable (as per CAMDEX classification) participants, supports the idea that it is not manifest disease that is driving age-related changes to brain structure.

Our study has some strengths and limitations. The use of a large independent healthy training dataset (N = 2001), on which the brain-predicted age values were based, allowed us to put brain ageing in DS in context of what is expected in during healthy ageing. However, one limitation of acquiring these data from various public sources is that we have inadequate demographic or behavioural data from which to quantify the characteristics of these individuals, other than that they were screened to be in good general and neurological health. The use of multi-modal neuroimaging (i.e., MRI and PET) to provide data on age-related brain changes in DS from independent sources also adds to the strength of the findings. A general caveat to consider when conducting neuroimaging analysis of individuals with DS is that when normalisation is required, as in this study, image registration performance may be reduced, as brain structure in DS is thought to be atypical. However, in this case, we used SPM DARTEL to perform highly accurate non-

linear registrations (Klein, et al., 2009) and if registration error had been driving the brain-PAD results, then this would increase noise and reduce the sensitivity to relate brain-PAD to external measures such as CAMCOG score. One perhaps surprising result is that the local controls in the study showed significantly ‘younger’ appearing brains, according to brain-PAD scores, relative to the independent training sample. This could potentially be driven by scanner effects, although by design the training sample include individuals from a range of different MRI scanner systems and field strengths in order to dilute any potential scanner biases that might cause overfitting and reduce generalisability. Another explanation could be a recruitment bias in that the local controls were comprised of individuals preferentially exposed to positive influences on apparent brain ageing, although steps were taken to recruit a wide spectrum of controls from beyond the confines of the University of Cambridge. We were unable to acquire detailed demographic or behavioural data on these individuals, so we were could not ascertain whether the variance in brain-PAD in controls related to any potential protective effects, such as increased years of education or physical exercise. Finally, as mentioned above, the cross-sectional nature of this study means that we cannot examine trajectories of change in people with DS, which would provide important information about the likelihood of future neurological decline and negative brain ageing.

## 5. Conclusions

This multi-modality neuroimaging study of DS indicates that one consequence of trisomy 21 is an increase in structural brain ageing, detectable in middle adulthood. While longitudinal studies are necessary to determine whether this increase in apparent brain ageing is static or accelerating, it is notable that the presence of PiB-binding was related to increased brain-PAD and that in DS participants with evidence of  $\beta$ -amyloid deposition, brain-PAD related to cognitive decline. It seems that some people with DS begin to show converging signs of potentially pathological deterioration, and that this can be detected using T1-weighted MRI to index individual differences in brain ageing. When no evidence of PIB-binding was observed, both brain ageing and cognitive performance remained unaffected. This could imply that amyloid-deposition, or related latent factor, could be driving the deleterious brain changes associated with ageing in DS.

## Acknowledgements

We would like to thank the PET imaging technologist, MR radiographers, technicians, and radiochemists at the Wolfson Brain Imaging Centre, along with the clinicians for their assistance in acquiring the data reported herein. We would particularly like to thank all participants with Down syndrome, their families and carers for their time and support of this research. James Cole is funded by a research grant to Imperial College London from the Medical Research Council (MR/L022141/1). The collection of the data reported in this paper was supported by a grant to the University of Cambridge from the Medical Research Council (Grant ID # 98480). Additional funding came from the NIHR Cambridge Biomedical Research centre, the NIHR Collaborations in Leadership for Applied Health Research and Care (CLAHRC) for the East of England, the NIHR Cambridge Dementia Biomedical Research Unit, the Down's Syndrome Association (DSA) and the Health Foundation. We are grateful for their support. The views expressed are those of the authors and not necessarily those of the NHS, the NIHR or the Department of Health.

## Disclosure statement

JHC reports no conflicts of interest.

TA, LRW, SHZ and AJH no conflict of interest.

RR no conflict of interest.

YTH, TDF and RS no conflict of interest.

JA-C, AC-B and PJN no conflict of interest.

DKM no conflict of interest.

## References

- Annus T, Wilson LR, Acosta-Cabronero J, Cardenas-Blanco A, Hong YT, Fryer TD, Coles JP, Menon DK, Zaman SH, Holland AJ, Nestor PJ. The Down syndrome brain in the presence and absence of fibrillar  $\beta$ -amyloidosis. *Neurobiol Aging* 2017. 53, 11-9.
- Annus T, Wilson LR, Hong YT, Acosta-Cabronero J, Fryer TD, Cardenas-Blanco A, Smith R, Boros I, Coles JP, Aigbirhio FI, Menon DK, Zaman SH, Nestor PJ, Holland AJ. The pattern of amyloid accumulation in the brains of adults with Down syndrome. *Alzheimer's & Dementia* 2016. 12(5), 538-45.
- Ashburner J. A fast diffeomorphic image registration algorithm. *Neuroimage* 2007. 38(1), 95-113.
- Avants BB, Tustison NJ, Song G, Cook PA, Klein A, Gee JC. A reproducible evaluation of ANTs similarity metric performance in brain image registration. *Neuroimage* 2011. 54(3), 2033-44.
- Ball SL, Holland AJ, Huppert FA, Treppner P, Watson P, Hon J. The modified CAMDEX informant interview is a valid and reliable tool for use in the diagnosis of dementia in adults with Down's syndrome. *J Intellect Disabil Res* 2004. 48(Pt 6), 611-20.
- Beacher F, Daly E, Simmons A, Prasher V, Morris R, Robinson C, Lovestone S, Murphy K, Murphy DG. Brain anatomy and ageing in non-demented adults with Down's syndrome: an in vivo MRI study. *Psychol Med* 2010. 40(4), 611-9.
- Braskie MN, Klunder AD, Hayashi KM, Protas H, Kepe V, Miller KJ, Huang SC, Barrio JR, Ercoli LM, Siddarth P, Satyamurthy N, Liu J, Toga AW, Bookheimer SY, Small GW, Thompson PM. Plaque and tangle imaging and cognition in normal aging and Alzheimer's disease. *Neurobiol Aging* 2010. 31(10), 1669-78.
- Busciglio J, Pelsman A, Wong C, Pigino G, Yuan M, Mori H, Yankner BA. Altered metabolism of the amyloid beta precursor protein is associated with mitochondrial dysfunction in Down's syndrome. *Neuron* 2002. 33(5), 677-88.
- Chowdhury MH, Nagai A, Bokura H, Nakamura E, Kobayashi S, Yamaguchi S. Age-related changes in white matter lesions, hippocampal atrophy, and cerebral microbleeds in healthy subjects without major cerebrovascular risk factors. *J Stroke Cerebrovasc Dis* 2011. 20(4), 302-9.
- Cole JH, Leech R, Sharp DJ, for the Alzheimer's Disease Neuroimaging I. Prediction of brain age suggests accelerated atrophy after traumatic brain injury. *Ann Neurol* 2015. 77(4), 571-81.
- Cole JH, Underwood J, Caan MWA, De Francesco D, van Zoest RA, Leech R, Wit FWNM, Portegies P, Geurtsen GJ, Schmand BA, Schim van der Loeff MF, Franceschi C, Sabin CA, Majoie CBLM, Winston A, Reiss P, Sharp DJ. Increased brain-predicted aging in treated HIV disease. *Neurology* 2017. <http://dx.doi.org/10.1212/wnl.0000000000003790>.
- Covelli V, Raggi A, Meucci P, Paganelli C, Leonardi M. Ageing of people with down's syndrome: A systematic literature review from 2000 to 2014. *Int J Rehabil Res* 2016. 39(1), 20-8.
- Devenny DA, Krinsky-McHale SJ, Sersen G, Silverman WP. Sequence of cognitive decline in dementia in adults with Down's syndrome. *J Intellect Disabil Res* 2000. 44(6), 654-65.
- Devenny DA, Wegiel J, Schupf N, Jenkins E, Zigman W, Krinsky-McHale SJ, Silverman WP. Dementia of the Alzheimer's type and accelerated aging in Down syndrome. *Sci Aging Knowledge Environ* 2005. 2005(14), dn1.
- Dosenbach NUF, Nardos B, Cohen AL, Fair DA, Power JD, Church JA, Nelson SM, Wig GS, Vogel AC, Lessov-Schlaggar CN, Barnes KA, Dubis JW, Feczko E, Coalson RS, Pruett JR, Barch DM, Petersen SE, Schlaggar BL. Prediction of Individual Brain Maturity Using fMRI. *Science* 2010. 329(5997), 1358-61.

- Fjell AM, Walhovd KB, Fennema-Notestine C, McEvoy LK, Hagler DJ, Holland D, Brewer JB, Dale AM. One-year brain atrophy evident in healthy aging. *J Neurosci* 2009. 29(48), 15223-31.
- Franke K, Gaser C. Longitudinal changes in individual BrainAGE in healthy aging, mild cognitive impairment, and Alzheimer's Disease. *GeroPsych* 2012. 25(4), 235-45.
- Franke K, Gaser C, Manor B, Novak V. Advanced BrainAGE in older adults with type 2 diabetes mellitus. *Front Aging Neurosci* 2013. 5, 90.
- Franke K, Ziegler G, Klöppel S, Gaser C. Estimating the age of healthy subjects from T1-weighted MRI scans using kernel methods: Exploring the influence of various parameters. *Neuroimage* 2010. 50(3), 883-92.
- Gaser C, Franke K, Klöppel S, Koutsouleris N, Sauer H. BrainAGE in Mild Cognitive Impaired Patients: Predicting the Conversion to Alzheimer's Disease. *PLoS One* 2013. 8(6).
- Gunn RN, Lammertsma AA, Hume SP, Cunningham VJ. Parametric imaging of ligand-receptor binding in PET using a simplified reference region model. *Neuroimage* 1997. 6(4), 279-87.
- Hartley SL, Handen BL, Devenny DA, Hardison R, Mihaila I, Price JC, Cohen AD, Klunk WE, Mailick MR, Johnson SC, Christian BT. Cognitive functioning in relation to brain amyloid- $\beta$  in healthy adults with Down syndrome. *Brain* 2014. 137(9), 2556-63.
- Head E, Lott IT, Wilcock DM, Lemere CA. Aging in down syndrome and the development of Alzheimer's disease neuropathology. *Current Alzheimer Research* 2016. 13(1), 18-29.
- Holland AJ, Hon J, Huppert FA, Stevens F, Watson P. Population-based study of the prevalence and presentation of dementia in adults with Down's syndrome. *Br J Psychiatry* 1998. 172, 493-8.
- Horvath S, Garagnani P, Bacalini MG, Pirazzini C, Salvioli S, Gentilini D, Di Blasio AM, Giuliani C, Tung S, Vinters HV, Franceschi C. Accelerated epigenetic aging in Down syndrome. *Aging Cell* 2015. 14(3), 491-5.
- Jack CR, Wiste HJ, Weigand SD, Rocca WA, Knopman DS, Mielke MM, Lowe VJ, Senjem ML, Gunter JL, Preboske GM, Pankratz VS, Vemuri P, Petersen RC. Age-specific population frequencies of cerebral  $\beta$ -amyloidosis and neurodegeneration among people with normal cognitive function aged 50-89 years: A cross-sectional study. *Lancet Neurol* 2014. 13(10), 997-1005.
- Jenkins EC, Velinov MT, Ye L, Gu H, Li S, Jenkins Jr EC, Brooks SS, Pang D, Devenny DA, Zigman WB, Schupf N, Silverman WP. Telomere shortening in T lymphocytes of older individuals with Down syndrome and dementia. *Neurobiol Aging* 2006. 27(7), 941-5.
- Jenkins EC, Ye L, Gu H, Ni SA, Velinov M, Pang D, Krinsky-McHale SJ, Zigman WB, Schupf N, Silverman WP. Shorter telomeres may indicate dementia status in older individuals with Down syndrome. *Neurobiol Aging* 2010. 31(5), 765-71.
- Jenkins EC, Ye L, Krinsky-Mchale SJ, Zigman WB, Schupf N, Silverman WP. Telomere longitudinal shortening as a biomarker for dementia status of adults with Down syndrome. *American Journal of Medical Genetics, Part B: Neuropsychiatric Genetics* 2016. 171(2), 169-74.
- Jovanovic SV, Clements D, MacLeod K. Biomarkers of oxidative stress are significantly elevated in Down syndrome. *Free Radic Biol Med* 1998. 25(9), 1044-8.
- Klein A, Andersson J, Ardekani BA, Ashburner J, Avants B, Chiang MC, Christensen GE, Collins DL, Gee J, Hellier P, Song JH, Jenkinson M, Lepage C, Rueckert D, Thompson P, Vercauteren T, Woods RP, Mann JJ, Parsey RV. Evaluation of 14 nonlinear deformation algorithms applied to human brain MRI registration. *Neuroimage* 2009. 46(3), 786-802.
- Koran ME, Hohman TJ, Edwards CM, Vega JN, Pryweller JR, Slosky LE, Crockett G, Villa de Rey L, Meda SA, Dankner N, Avery SN, Blackford JU, Dykens EM, Thornton-Wells TA. Differences in age-related

effects on brain volume in Down syndrome as compared to Williams syndrome and typical development. *J Neurodev Disord* 2014. 6(1), 8.

Koutsouleris N, Davatzikos C, Borgwardt S, Gaser C, Bottlender R, Frodl T, Falkai P, Riecher-Rössler A, Möller H-J, Reiser M, Pantelis C, Meisenzahl E. Accelerated Brain Aging in Schizophrenia and Beyond: A Neuroanatomical Marker of Psychiatric Disorders. *Schizophr Bull* 2013.

Krasuski JS, Alexander GE, Horwitz B, Rapoport SI, Schapiro MB. Relation of medial temporal lobe volumes to age and memory function in nondemented adults with Down's syndrome: implications for the prodromal phase of Alzheimer's disease. *Am J Psychiatry* 2002. 159(1), 74-81.

Lao PJ, Betthausen TJ, Hillmer AT, Price JC, Klunk WE, Mihaila I, Higgins AT, Bulova PD, Hartley SL, Hardison R, Tumuluru RV, Murali D, Mathis CA, Cohen AD, Barnhart TE, Devenny DA, Mailick MR, Johnson SC, Handen BL, Christian BT. The effects of normal aging on amyloid- $\beta$  deposition in nondemented adults with Down syndrome as imaged by carbon 11-labeled Pittsburgh compound B. *Alzheimer's and Dementia* 2016. 12(4), 380-90.

Lopez-Otin C, Blasco MA, Partridge L, Serrano M, Kroemer G. The hallmarks of aging. *Cell* 2013. 153(6), 1194-217.

Luders E, Cherbuin N, Gaser C. Estimating brain age using high-resolution pattern recognition: Younger brains in long-term meditation practitioners. *Neuroimage* 2016. 134, 508-13.

Mann DM, Esiri MM. The pattern of acquisition of plaques and tangles in the brains of patients under 50 years of age with Down's syndrome. *J Neurol Sci* 1989. 89(2-3), 169-79.

Margallo-Lana ML, Moore PB, Kay DWK, Perry RH, Reid BE, Berney TP, Tyrer SP. Fifteen-year follow-up of 92 hospitalized adults with Down's syndrome: Incidence of cognitive decline, its relationship to age and neuropathology. *J Intellect Disabil Res* 2007. 51(6), 463-77.

Melville CA, Cooper SA, McGrother CW, Thorp CF, Collacott R. Obesity in adults with Down syndrome: A case-control study. *J Intellect Disabil Res* 2005. 49(2), 125-33.

Muller M, Appelman APA, van der Graaf Y, Vincken KL, Mali WP, Geerlings MI. Brain atrophy and cognition: Interaction with cerebrovascular pathology? *Neurobiol Aging* 2011. 32(5), 885-93.

Mullins D, Daly E, Simmons A, Beacher F, Foy CML, Lovestone S, Hallahan B, Murphy KC, Murphy DG. Dementia in Down's syndrome: an MRI comparison with Alzheimer's disease in the general population. *J Neurodev Disord* 2013. 5(1), 19-.

Mwangi B, Hasan KM, Soares JC. Prediction of individual subject's age across the human lifespan using diffusion tensor imaging: A machine learning approach. *Neuroimage* 2013. 75(0), 58-67.

Nelson LD, Siddarth P, Kepe V, Scheibel KE, Huang SC, Barrio JR, Small GW. Positron emission tomography of brain  $\beta$ -amyloid and tau levels in adults with down syndrome. *Arch Neurol* 2011. 68(6), 768-74.

Oliver C, Crayton L, Holland A, Hall S, Bradbury J. A four year prospective study of age-related cognitive change in adults with Down's syndrome. *Psychol Med* 1998. 28(6), 1365-77.

Patenaude B, Smith SM, Kennedy DN, Jenkinson M. A Bayesian model of shape and appearance for subcortical brain segmentation. *Neuroimage* 2011. 56(3), 907-22.

Phillips AC, Sleigh A, McAllister CJ, Brage S, Carpenter TA, Kemp GJ, Holland AJ. Defective Mitochondrial Function In Vivo in Skeletal Muscle in Adults with Down's Syndrome: A (31)P-MRS Study. *PLoS One* 2013. 8(12), e84031.

Pinter JD, Eliez S, Schmitt JE, Capone GT, Reiss AL. Neuroanatomy of Down's syndrome: a high-resolution MRI study. *Am J Psychiatry* 2001. 158(10), 1659-65.

- R Core Team. 2015. R: A language and environment for statistical computing. R Foundation for Statistical Computing, Vienna, Austria.
- Rodrigue KM, Kennedy KM, Devous Sr MD, Rieck JR, Hebrank AC, Diaz-Arrastia R, Mathews D, Park DC.  $\beta$ -amyloid burden in healthy aging: Regional distribution and cognitive consequences. *Neurology* 2012. 78(6), 387-95.
- Romano A, Cornia R, Moraschi M, Bozzao A, Chiacchiararelli L, Coppola V, Iani C, Stella G, Albertini G, Pierallini A. Age-Related Cortical Thickness Reduction in Non-Demented Down's Syndrome Subjects. *J Neuroimaging* 2016. 26(1), 95-102.
- Ronan L, Alexander-Bloch AF, Wagstyl K, Farooqi S, Brayne C, Tyler LK, Fletcher PC. Obesity associated with increased brain age from midlife. *Neurobiol Aging* 2016. 47, 63-70.
- Roth GM, Sun B, Greensite FS, Lott IT, Dietrich RB. Premature aging in persons with Down syndrome: MR findings. *AJNR Am J Neuroradiol* 1996. 17(7), 1283-9.
- Rumble B, Retallack R, Hilbich C, Simms G, Multhaup G, Martins R, Hockey A, Montgomery P, Beyreuther K, Masters CL. Amyloid A4 protein and its precursor in Down's syndrome and Alzheimer's disease. *N Engl J Med* 1989. 320(22), 1446-52.
- Schnack HG, Haren NEMv, Nieuwenhuis M, Pol HEH, Cahn W, Kahn RS. Accelerated Brain Aging in Schizophrenia: A Longitudinal Pattern Recognition Study. *Am J Psychiatry* 2016. 173(6), 607-16.
- Steffener J, Habeck C, O'Shea D, Razlighi Q, Bherer L, Stern Y. Differences between chronological and brain age are related to education and self-reported physical activity. *Neurobiol Aging* 2016. 40, 138-44.
- Teipel SJ, Alexander GE, Schapiro MB, Möller HJ, Rapoport SI, Hampel H. Age-related cortical grey matter reductions in non-demented Down's syndrome adults determined by MRI with voxel-based morphometry. *Brain* 2004. 127(4), 811-24.
- Tiano L, Busciglio J. Mitochondrial dysfunction and Down's syndrome: Is there a role for coenzyme Q10? *Biofactors* 2011. 37(5), 386-92.
- Vaziri H, Schächter F, Uchida I, Wei L, Zhu X, Effros R, Cohen D, Harley CB. Loss of telomeric DNA during aging of normal and trisomy 21 human lymphocytes. *Am J Hum Genet* 1993. 52(4), 661-7.
- Wang PP. A neuropsychological profile of Down syndrome: Cognitive skills and brain morphology. *Mental Retardation and Developmental Disabilities Research Reviews* 1996. 2(2), 102-8.
- Wardlaw JM, Smith EE, Biessels GJ, Cordonnier C, Fazekas F, Frayne R, Lindley RI, O'Brien JT, Barkhof F, Benavente OR, Black SE, Brayne C, Breteler M, Chabriat H, DeCarli C, de Leeuw FE, Doubal F, Duering M, Fox NC, Greenberg S, Hachinski V, Kilimann I, Mok V, Oostenbrugge RV, Pantoni L, Speck O, Stephan BCM, Teipel S, Viswanathan A, Werring D, Chen C, Smith C, van Buchem M, Norrving B, Gorelick PB, Dichgans M. Neuroimaging standards for research into small vessel disease and its contribution to ageing and neurodegeneration. *Lancet Neurol* 2013. 12(8), 822-38.
- Wilcock DM, Schmitt FA, Head E. Cerebrovascular contributions to aging and Alzheimer's disease in Down syndrome. *Biochimica et Biophysica Acta - Molecular Basis of Disease* 2016. 1862(5), 909-14.
- Wisniewski KE, Wisniewski HM, Wen GY. Occurrence of neuropathological changes and dementia of Alzheimer's disease in Down's syndrome. *Ann Neurol* 1985. 17(3), 278-82.
- Zigman WB. Atypical aging in down syndrome. *Developmental Disabilities Research Reviews* 2013. 18(1), 51-67.